Bull. Chem. Soc. Ethiop. 1998, 12(1), 69-77. ISSN 1011-3294
Printed in Ethiopia

STUDIES OF THE DOUBLE LAYER AT THE WATER/*o*-NITROTOLUENE INTERFACE

Hailemichael Alemu*, B. Hundhammer and Theordos Solomon

Department of Chemistry, Addis Ababa University, P.O. Box 1176, Addis Ababa, Ethiopia

(Received April 2, 1998)

ABSTRACT. The structure of the electrical double layer at the water/*o*-nitrotoluene interface containing different base electrolytes with different concentrations has been studied by impedance measurements. The capacitance values obtained from experiments have been compared with the values calculated from the Gouy-Chapman theory. Analysis of the results has indicated the absence of specific adsorption at the water/*o*-nitrotoluene interface.

INTRODUCTION

The electrical double-layer at the interface between two immiscible electrolyte solutions (ITIES) has been investigated by many workers using various electrochemical methods (see references 1, 2 and 3 and references cited therein). The most frequently used technique is the ac impedance measurement. Such studies have so far been made mainly on the water/nitrobenzene and water/1,2-dichloroethane interfaces. The quantity that can be obtained from the impedance measurements and which is related to the double layer structure is the interfacial capacitance. Extension of such studies to other solvent systems seems to be very important since it can contribute to the general understanding of the structure of the electrical double-layer at liquid/liquid interfaces.

In the present investigation, the electrical double-layer at the water/*o*-nitrotoluene interface has been studied using different types of supporting electrolytes. The double-layer capacitances were measured at different concentrations using ac impedance technique. The results are compared with those of the water/nitrobenzene and the water/1,2-dichloroethane interfaces.

EXPERIMENTAL

The electronic set-up used for the impedance measurements is represented by the block diagram in Figure 1. A four electrode potentiostat with automatic IR compensation similar to that described in ref. 4 was constructed and employed. To regulate the proper compensation of the ohmic drop across the interface, the current output of the potentiostat was connected to an oscilloscope (Tektronix Model 501). The superimposed sinusoidal potential was of magnitude $\Delta E = 5$ mV peak to peak and was fed from a frequency generator (Tektronix FG 501) while the triangular voltage ramp (5 mV/s) was generated using MP-1502 Electroanalyzer (McKee Pederson Instruments). The current output of the potentiostat was connected to the input of a lock-in analyzer (PAR Model 5204) which was used for the continuous measurements of the in-phase and quadrature components of the ac-current. The outputs were detected using the storage oscilloscope and X-Y recorder. The real and imaginary parts of the impedance were then calculated from the in-phase and quadrature components by means of standard procedures [5] and using personal computer. The electrochemical cell and the reference electrodes used were the same as those described in ref. 6.

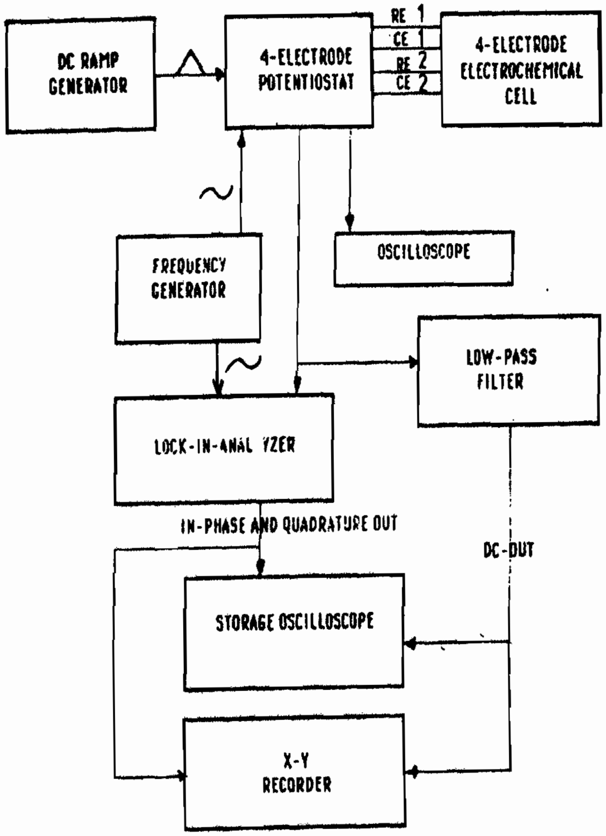

Figure 1. Block diagram of the electrical set-up used for impedance measurements.

Tetrabutylammonium tetraphenylborate (TBATPB) (Fluka, 99%) was used as received. μ-Nitrido-bis (triphenylphosphorous)3,3-como-bis(undecahydro-1,2-dicarba-3-cobalta-closododecabor)ate (PNPDCC) was prepared as described in ref. 7. Li_2SO_4 (BDH), LiCl (Fluka, water free), and LiF (BDH) were recrystallized from their super saturated aqueous solutions. *o*-Nitrotoluene (MERCK, Schuchardt) was purified using the method given in ref. 8. All aqueous electrolyte solutions were prepared from all-glass doubly distilled water. The organic and the aqueous phases were equilibrated with each other before the starting of each experiment. All measurements were made at a laboratory temperature of 22±1 °C.

RESULTS AND DISCUSSION

Impedance measurements were carried out within a potential range where charge transfer can be neglected. The in-phase and quadrature components of the ac current were recorded as a function of potential at a given frequency. This was repeated for different frequencies. The results were transformed into real Z' and imaginary Z" parts of the complex impedance Z from which Z_c was calculated using standard procedures [5]. Linear relationships were obtained on plotting Z_c *vs* ω^{-1} at different potentials. From the slops of the plots the values of the interfacial capacity C were evaluated as a function of potential. Further details are available in ref. 9. For comparison the capacitance values of the diffuse double layer, C_d were computed from the Gouy-Chapman theory.

Using the Gouy-Chapman relationship for a symmetrical (z : z) electrolyte the surface charge densities are [1, 10, 11]

$$q^w = -2A^w \sinh(ZF\Delta\Phi^w_2/2RT) \qquad (1)$$

$$q^o = -2A^o \sinh(ZF\Delta\Phi^o_2/2RT) \qquad (2)$$

and

$$A^{w(o)} = (2RT\varepsilon^{w(o)}C^o)^{½} \qquad (3)$$

where $\varepsilon^{w(o)}$ is the permitivity of the solvent, and the capacity of the diffuse layer of each phase is:

$$C_w = -\,\delta q^w/\delta\Delta\Phi^w_2 = (ZFA^w/RT)\cosh(ZF\Delta\Phi^w_2/2RT) \qquad (4)$$

$$C_o = -\,\delta q^o/\delta\Delta\Phi^o_2 = (ZFA^o/RT)\cosh(ZF\Delta\Phi^o_2/2RT) \qquad (5)$$

and

$$1/C_d = 1/C_w + 1/C_o \qquad (6)$$

Figure 2 shows the plots of the interfacial capacity C as a function of potential at various electrolyte (LiCl(w) / TBATPB(o)) concentrations. Included in the figure are the plots of the diffuse double-layer C_d *vs* potential calculated from the Gouy-Chapman theory. As seen from this figure there is good agreement between the experimental and the calculated capacitance values at low electrolyte concentrations (5 and 10 mM). However, at high concentration the experimental capacity is lower than the C_d predicted from theory. It is known that the Gouy-Chapman treatment of the diffuse double-layer is adequate at low ionic concentration but may become progressively more imprecise as the concentration increases to the 0.1-1.0 M level [12].

Comparison of Figure 2 with Figure 3 illustrates the decrease in the interfacial capacitance when PNPDCC was used as the organic base electrolyte. The difference in the magnitude of the capacitance minima when PNPDCC is substituted for TBATPB increases with increasing electrolyte concentrations (1.75, 2.08, 3.69 μF cm^{-2} for 5, 10, 50 mM, respectively). As shown in the figures, the use of PNPDCC has enabled the capacitance measurements to be carried out over a wider potential range.

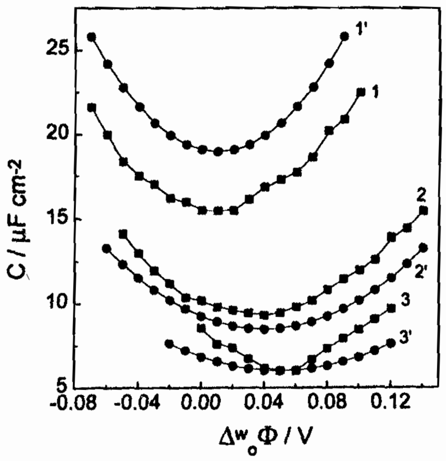

Figure 2. Plots of the experimental (■) and theoretical (●) interfacial capacitance C *vs* $\Delta^w_o\Phi$ for the system LiCl(w)/TBATPB(o-nt). Electrolyte concentration: 50 mM (1,1'); 10 mM (2,2'); and 5 mM (3,3').

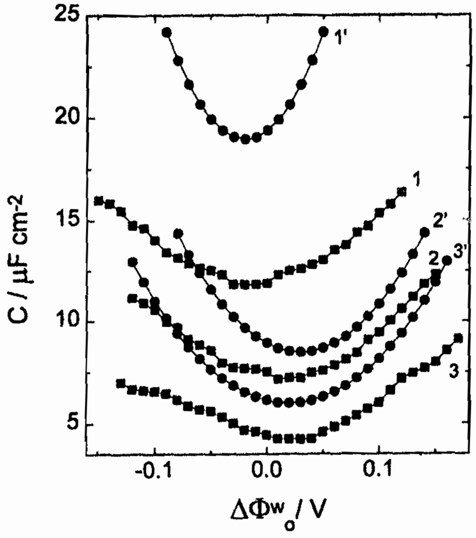

Figure 3. Plots of the experimental (■) and theoretical (●) interfacial capacitance C *vs* $\Delta^w_o\Phi$ for the system LiCl(w)/PNPDCC(o-nt). Electrolyte concentration: 50 mM (1,1'); 10 mM (2,2'); and 5 mM (3,3').

It can be seen from Figure 2 that the potential of the capacitance minimum for low electrolyte concentrations ($C^o = 5$ and 10 mM) occurs at about $\Delta^w_o\Phi = 0.05$ V. The minimum shifts towards negative potentials with an increase in electrolyte concentration.

The same kind of shift is observed when TBATPB is substituted by PNPDCC. A similar behaviour was reported by Senda *et al.* [13] for the system LiCl in water and TBATPB in nitrobenzene. These authors tested for the existence of specific ionic adsorption, and their results indicated the absence of specific adsorption. In the classical treatment of the double layer at the mercury/electrolyte solution interface, a shift in the potential of zero charge with increase in electrolyte concentration (Esin-Markov effect) is a characteristic feature of the existence of specific ionic adsorption [12, 14]. Thus, in order to detect the existence of specific adsorption at the water/*o*-nitrotoluene interface, the Eisen-Markov coefficient was calculated by plotting the potential as a function of the logarithm of the electrolyte activity at constant charge density.

Assuming no specific adsorption, one obtains for the Esin-Markov coefficient [12, 14],

$$(\delta\Delta\Phi^{w}{}_{2}/\delta \ln a\pm_{TBATPB}{}^{o\text{-}NT})_{qw,\mu j \neq TBATPB} = -RT/F(1 + q^{w}/2)[(q^{w}/2)^{2} + (A^{o\text{-}NT})^{2}]^{½}) \qquad (7)$$

where $A^{o\text{-}NT} = (2RT\varepsilon^{o\text{-}NT}C_{TBA+})$.

Accordingly, the coefficient of the above equation should reduce to -2RT/F, -RT/F, and 0 when $q^{w} \gg 0$, $q^{w} = 0$, and $q^{w} \ll 0$, respectively. The Esin-Markov plots at several constant q^{w} values for TBATPB and PNPDCC in *o*-nitrotoluene are shown in Figures 4 and 5, respectively. It can be noted from these figures that the slopes of $\Delta\Phi^{w}{}_{0}$ *vs* lna± are closer to zero with increasing negative charges (for TBATPB slope = -0.006, and -0.001 V for q^{w} = -0.3, and -0.5 μC cm^{-2}, respectively, and for PNPDCC slope = -0.003, and -0.001 V for q^{w} = -0.5, and -1.0 μC cm^{-2}, respectively). This is in very good agreement with the above equation. It can also be seen from Figure 5 that the slopes for positive charges increase negatively and approach the limiting value -0.050 V (slope = 0.046 V for q^{w} = 0.9 μC cm^{-2}) which is consistent with the prediction of equation 7. A similar increase is also apparent in Figure 4; however, the experimental values of q^{w} for TBATPB were not large enough to reach the limiting value. At the potential of zero charge, Figures 4 and 5 have slopes of -0.017 and -0.016 V, respectively. These values are close to the expected theoretical value (RT/F = -0.025 V).

The above results indicate the apparent absence of specific adsorption for the aqueous salt LiCl and the organic salt TBATPB or PNPDCC in the concentration range and the potential range studied. Thus, the observed shift in the potential of the capacitance minimum with concentration was not due to specific adsorption.

Figures 6 and 7 show the plot of the inverse capacitance C^{-1} of the interface as a function of the inverse capacitance C_{d}^{-1} of the diffuse double layer at different constant charge densities (q^{w}). C_{d} was obtained from the Gouy-Chapman theory. The solid line in each figure is the plot at $q^{w} = 0$.

The plots seem to satisfy the equation,

$$1/C = 1/C_{d} + 1/C_{i} \qquad (8)$$

The plot of $1/C$ *vs* $1/C_{d}$ at constant q is used as an alternative criterion for checking the existence of specific adsorption in the classical treatment of the double-layer [12, 14].

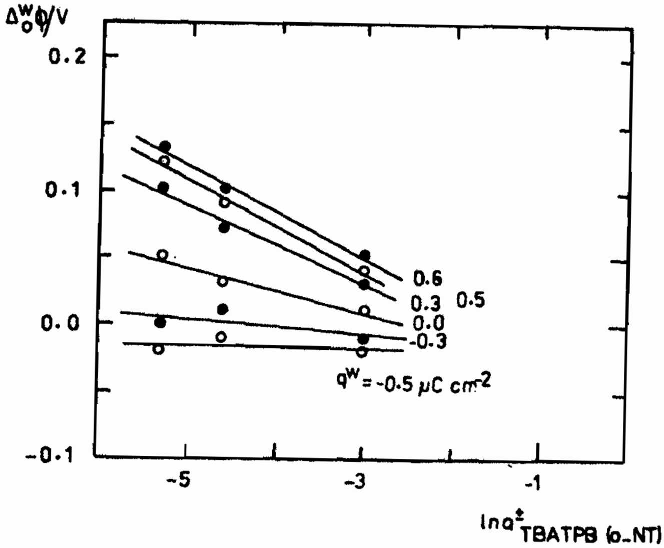

Figure 4. Esin-Markov plots for the solutions of TBATPB in *o*-nitrotoluene in contact with aqueous solution of LiCl.

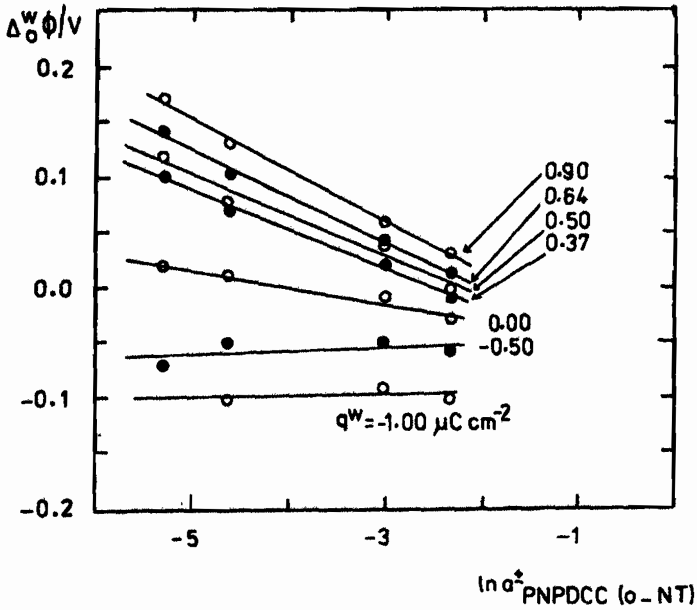

Figure 5. Esin-Markov plots for the solutions of PNPDCC in *o*-nitrotoluene in contact with aqueous solution of LiCl.

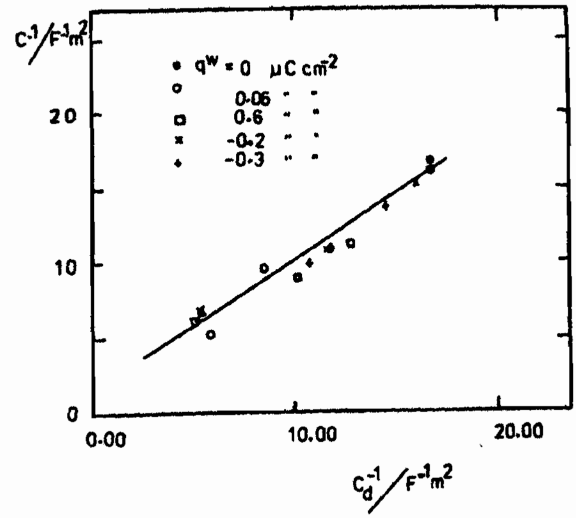

Figure 6. Inverse capacitance C^{-1} *vs* C_d^{-1} for the system LiCl(w)/TBATPB(*o*-nt) at different electrolyte concentrations (C^o = 5, 10 and 50 mM) and at constant charge densities. The line is for q^w=0 μC cm^{-2}.

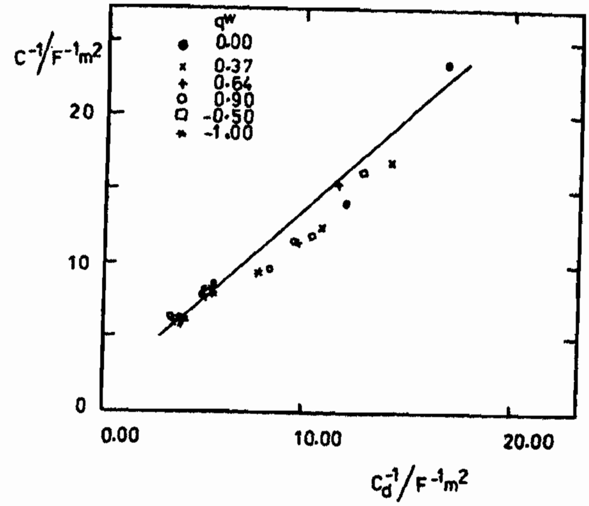

Figure 7. Inverse capacitance C^{-1} *vs* C_d^{-1} for the system LiCl(w)/PNPDCC(*o*-nt) at different electrolyte concentrations (C^o = 5, 10, 50 and 100 mM) and at constant charge densities. The line is for q^w=0 μC cm^{-2}.

At $q^w = 0$ the value of $1/C_i$ as determined from the intercept are 1.35 and 1.32 $F^{1}m^{2}$ for LiCl(w)/TBATPB(*o*-NT) and LiCl(w)/PNPDCC(*o*-NT), respectively. These correspond to C_i values of 74 and 76 μF cm^{-2}, respectively. The similarity in the C_i values indicate that the structure of the inner layer of the interface remains unaffected when TBATPB is replaced by PNPDCC. Furthermore, these values are comparable with the one obtained for the water/nitrobenzene interface in which C_i = 80 μF cm^{-2} as estimated from the differential capacity of the interface using LiCl(w) and TBATPB(o) as base electrolytes [15].

Capacitance *vs* potential curves for the system LiCl, LiF and Li_2SO_4 in water, and PNPDCC in the organic phase are shown in Figure 8. A comparison of the curves in Figure 8 shows that the values of the capacitance minimum for SO_4^{2-} is lower than those of Cl^- and F^- by about 1.2 μF cm^{-2}. It is also apparent that the potential of the capacitance minimum for SO_4^{2-} corresponds to $\Delta^{w}_{o}\Phi = 0$ V.

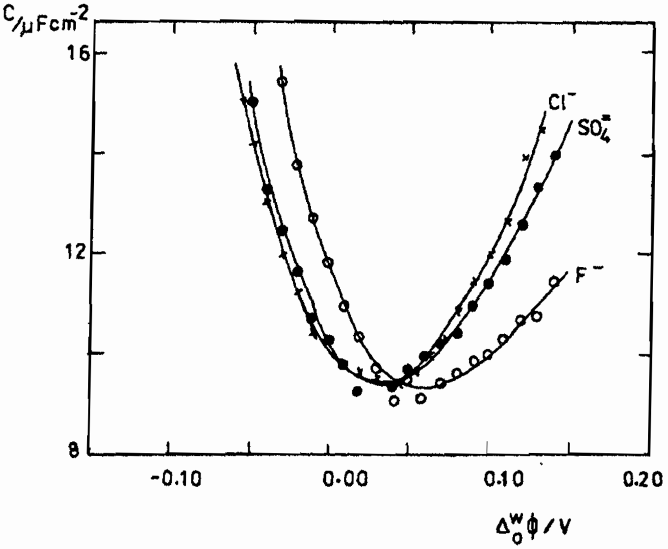

Figure 8. Plots of the interfacial capacitance C *vs* $\Delta^{w}_{o}\Phi$ for the water/*o*-nitrotoluene interface containing 10 mM LiCl, LiF and Li_2SO_4 in the aqueous phase, respectively, and 10 mM PNPDCC in the organic phase.

In summary no specific ionic adsorption was observed for the studied electrolytes and in many respects the behaviour of the water/*o*-nitrotoluene interface has been found to be similar to that of the water/nitrobenzene interface.

REFERENCES

1. Marecek, V.; Samec, Z.; Koryta, J. *Advances in Colloid and Interface Science* **1988**, 29, 1.
2. Girault, H.H.; Schiffrin, D.J. *Electroanalytical Chemistry*, Vol. 15, Bard, A.J. (Ed.), Marcel Dekker: New York; 1989.
3. Samec, Z. *Chem. Rev.* **1988**, 88, 617.

4. Samec, Z.; Marecek, V.; Weber, J. *J. Electroanal. Chem.* **1979**, 100, 841.
5. Marecek, V.; Samec, Z. *J. Electroanal. Chem.* **1985**, 185, 263.
6. Alemu, H.; Hundhammer, B.; Solomon, T. *J. Electroanal. Chem.* **1990**, 294, 165.
7. Hundhammer, B.; Wilke, S. *J. Electroanal. Chem.* **1989**, 266, 133.
8. Riddick, J.A.; Bunger, W.B. *Organic Solvents*, Wiley Interscience; New York; 1986.
9. Alemu, H. Ph.D. Thesis, Addis Ababa University; 1991.
10. Samec, Z.; Marecek, V.; Homolka, D. *J. Electroanal. Chem.* **1981**, 126, 121.
11. Reid, J.D.; Vanysek, P.; Buck, R.P. *J. Electroanal. Chem.* **1984**, 161, 1.
12. Reeves, R. *Comprehensive Treatise of Electrochemistry*, Vol. 1, Bockris, J.; Conway, B.; Yeager, E. (Eds.), Plenum Press: New York; 1980, p 83.
13. Kakiuchi, T.; Senda, M. *Bull. Chem. Soc. Jpn.* **1983**, 56, 1753.
14. Mohilner, D.M. *Electroanalytical Chemistry*, Vol. 1, Bard, A.J. (Ed.), Marcel Dekker: New York; 1966, p 241.
15. Samec, Z.; Marecek, V.; Homolka, D. *J. Electroanal. Chem.* **1985**, 187, 31.